

## Relativistic algorithm for time transfer in Mars missions under IAU Resolutions: an analytic approach \*

Jun-Yang Pan<sup>1</sup> and Yi Xie<sup>1,2</sup>

<sup>1</sup> School of Astronomy and Space Science, Nanjing University, Nanjing 210093, China;  
[yixie@nju.edu.cn](mailto:yixie@nju.edu.cn)

<sup>2</sup> Key Laboratory of Modern Astronomy and Astrophysics, Nanjing University, Ministry of Education, Nanjing 210093, China

Received 2014 May 4; accepted 2014 June 12

**Abstract** With tremendous advances in modern techniques, Einstein’s general relativity has become an inevitable part of deep space missions. We investigate the relativistic algorithm for time transfer between the proper time  $\tau$  of the onboard clock and the Geocentric Coordinate Time, which extends some previous works by including the effects of propagation of electromagnetic signals. In order to evaluate the implicit algebraic equations and integrals in the model, we take an analytic approach to work out their approximate values. This analytic model might be used in an onboard computer because of its limited capability to perform calculations. Taking an orbiter like Yinghuo-1 as an example, we find that the contributions of the Sun, the ground station and the spacecraft dominate the outcomes of the relativistic corrections to the model.

**Key words:** reference systems — time — method: analytical — space vehicles

### 1 INTRODUCTION

With tremendous advances in modern techniques, Einstein’s general relativity (GR) has become an inevitable part of deep space missions. It has gone far beyond theoretical astronomy and physics into practice and engineering (Nelson 2011). Effects due to GR clearly showed up in the radio signals of some space missions (e.g. Bertotti et al. 2003; Jensen & Weaver 2007), which provide the tightest constraint on GR (Bertotti et al. 2003). However, Kopeikin et al. (2007) pointed out that the test of GR by the *Cassini* spacecraft (Bertotti et al. 2003) is under a restrictive condition that the Sun’s gravitational field is static, and if this restriction is removed the test becomes less stringent.

In GR, one important idea is to abandon the concept of Newton’s absolute time. There exist different kinds of times: proper time and coordinate times (Misner et al. 1973; Landau & Lifshitz 1975). Theoretically, the readings of an ideal clock form the proper time  $\tau$ , which is an observable and is associated with the clock itself. In fact, there is not an ideal clock. An atomic clock approaches an ideal clock with some finite error. However, even if an atomic clock were ideal, we still have to hypothesize that it reads the proper time. This is because GR is a geometric theory but an atomic

---

\* Supported by the National Natural Science Foundation of China.

clock is a quantum mechanical device, not governed by geometry but by the laws of quantum mechanics, which are still not geometrized. The coordinate times cannot be measured directly, but they might be used as variables in the equations of motion of celestial and artificial bodies and light rays. Coordinate times are connected with the proper time through the four-dimensional space-time interval, whose mathematical expression depends on kinematics and dynamics of the clock. This dramatically changes the way clocks are synchronized and the associated time transfer (see Petit & Wolf 2005; Nelson 2011, for reviews and references therein). Experiments involving time/frequency transfer might be used for testing theories of gravity (e.g. Samain 2002; Cacciapuoti & Salomon 2009; Wolf et al. 2009; Christophe et al. 2009, 2012; Deng & Xie 2013a,b, 2014).

In exploration missions to Mars and other planets, synchronization between the clock onboard a spacecraft and a clock on the ground is critical for control, navigation and scientific operation. According to International Astronomical Union (IAU) Resolutions (Soffel et al. 2003), two intermediate steps are required. *Step 1* is to relativistically transform onboard  $\tau$  to the Barycentric Coordinate Time (TCB), which is the global time of the solar system. Then, in *Step 2*, TCB is converted to the Geocentric Coordinate Time (TCG), which is the coordinate time belonging to the local reference system of the Earth. Then, TCG can be easily changed to other time scales associated with Earth, such as Terrestrial Time (TT), International Atomic Time (TAI) and Coordinated Universal Time (UTC).

Taking the Yinghuo-1 mission (Ping et al. 2010a,b) as a technical example of future Chinese Mars explorations, some works have been devoted to investigating *Step 1* and *Step 2*. Deng (2012) studied the transformation of *Step 1* by analytic and numerical methods and found two main effects: the gravitational field of the Sun and the velocity of the spacecraft in the Barycentric Celestial Reference System (BCRS). The combined contribution of these two effects can reach a few sub-seconds in one year (Deng 2012). Pan & Xie (2013) took clock offset into account in *Step 1* and found that if an onboard clock can be calibrated to achieve an accuracy better than  $\sim 10^{-6} - 10^{-5}$  s in one year (depending on the type of clock offset), the relativistic transformation between  $\tau$  and TCB will need to be carefully handled. Pan & Xie (2014) investigated the relativistic transformation between  $\tau$  and TCG, which combines *Step 1* and *Step 2*. It was found that the difference between  $\tau$  and TCG can reach the level of about 0.2 seconds in a year and if the threshold of 1 microsecond ( $\mu\text{s}$ ) is adopted, this transformation must include the effects due to the Sun, Venus, the Moon, Mars, Jupiter, Saturn and the velocities of the spacecraft and the Earth.

In this paper, we will include the effects of light propagation in the relativistic algorithm of time transfer for Mars missions under IAU Resolutions. More specifically, the relativistic time transfer connecting two time scales is carried out by the transmission of electromagnetic signals, which might be encoded with necessary information and commands. This also means the time scale in the present work is about  $10^3$  seconds, which is the light propagation time from a ground station to a Mars orbiter. The effects of the propagation of signals are absent in the previous works (Deng 2012; Pan & Xie 2013, 2014) and the time scale of one year in these works is much longer than the one we focus on here. For an orbiter around Mars, which has an orbit like Yinghuo-1's, we will develop an analytic model for such a procedure of time transfer. This analytic approach means all of the algebraic equations and integrals in the model will be solved and evaluated in some ways with sufficient approximations. Such an algorithm might be adopted for an onboard processor with limited capability to perform computation. The validity of this analytic approach needs to be checked independently and such a check will be our next goal.

In Section 2, we will establish a general model of relativistic time transfer between  $\tau$  and TCG for a Mars orbiter according to IAU Resolutions (Soffel et al. 2003). This model includes the effects of signal transmission from a station to a spacecraft. Implicit algebraic equations and integrals in the model will be approximately solved and evaluated in Section 3. In Section 4, by assuming an Yinghuo-1-like mission, we will calculate and show the contributions from various sources in this analytic model. Conclusions and discussion will be presented in Section 5.

## 2 GENERAL MODEL OF TIME TRANSFER BETWEEN $\tau$ AND TCG

In the framework of IAU Resolutions (Soffel et al. 2003), a clock onboard an orbiter (hereafter “P”) around Mars measures its own proper time  $\tau$  and a station (hereafter “S”) on the surface of the Earth can have its coordinate time  $T$  in TCG, which can be calculated from other well-maintained time scales, such as TT. In order to synchronize the onboard  $\tau$  with  $T$  on the Earth, S emits an electromagnetic signal encoded with some necessary information at time  $t_E$  in TCB and P receives the signal at time  $t_R$  in TCB. In this context, we can find the relation between these times as (e.g. Kopeikin et al. 2011)

$$\frac{d\tau}{dT} = \frac{d\tau}{dt_R} \frac{dt_R}{dt_E} \frac{dt_E}{dT}, \quad (1)$$

where the first term describes the transformation between  $\tau$  and TCB, the second term accounts for the propagation of the electromagnetic signal from S to P and the third term is the transformation between TCB and TCG.

The relativistic 4-dimensional transformation between  $\tau$  and the TCB in Equation (1) reads as (Soffel et al. 2003)

$$\frac{d\tau}{dt_R} = 1 - \epsilon^2 \left[ \bar{U}(\mathbf{x}_P) + \frac{1}{2} \mathbf{v}_P^2 \right] + \mathcal{O}(\epsilon^4). \quad (2)$$

Here,  $\epsilon = c^{-1}$  and  $c$  is the speed of light.  $\bar{U}(\mathbf{x}_P)$  is the Newtonian gravitational potential evaluated at the position of the spacecraft  $\mathbf{x}_P$  and  $\mathbf{v}_P$  is the velocity of the spacecraft in the BCRS. The potential can be decomposed further as  $\bar{U} = \sum_A \bar{U}_A$ , where the index “A” enumerates each body whose gravitational effect needs to be considered. Focusing on a spacecraft like Yinghuo-1, Deng (2012) and Pan & Xie (2013) studied its effects on the time transfer. The relativistic transformation between TCB and TCG in Equation (1) is (Soffel et al. 2003)

$$\frac{dt_E}{dT} = 1 + \epsilon^2 \left\{ \bar{U}(\mathbf{x}_\oplus) + \frac{1}{2} \mathbf{v}_\oplus^2 + \frac{d}{dT} \left[ \mathbf{v}_\oplus \cdot (\mathbf{x}_S - \mathbf{x}_\oplus) \right] \right\} + \mathcal{O}(\epsilon^4), \quad (3)$$

where  $\mathbf{x}_S$  and  $\mathbf{x}_\oplus$  are respectively the positions of the station and the geocenter in the BCRS and both of them are functions of  $t_E$ .

The second term in Equation (1), which describes the propagation of the signal, can be obtained from the relativistic light ray equations (see chap. 7 in Kopeikin et al. 2011, for details) and, thus, we can have (Moyer & Yuen 2000; Kopeikin et al. 2011)

$$\Delta t \equiv t_R - t_E = \Delta t_1 + \Delta t_2 + \mathcal{O}(\epsilon^4), \quad (4)$$

where

$$\Delta t_1 \equiv \epsilon f_1 = \epsilon |\mathbf{x}_P(t_R) - \mathbf{x}_S(t_E)|, \quad (5)$$

$$\Delta t_2 \equiv \epsilon^3 f_2 = 2\epsilon^3 G \sum_A m_A \ln \left[ \frac{r_{RA} + \hat{\mathbf{n}} \cdot \mathbf{r}_{RA}}{r_{EA} + \hat{\mathbf{n}} \cdot \mathbf{r}_{EA}} \right]. \quad (6)$$

Here,  $\Delta t_1$  is the Euclidean geometric effect and  $\Delta t_2$  is the Shapiro time delay (Shapiro 1964). In terms of  $\Delta t_1$ ,  $\mathbf{x}_P$  and  $\mathbf{x}_S$  depend respectively on  $t_R$  and  $t_E$ . In terms of  $\Delta t_2$ , we ignore the motions of all the gravitational bodies. Such a treatment is only valid when the time scale of light propagation is much less than the time scales of orbital motions of celestial bodies. This condition is satisfied in our investigation of a Mars mission because the light propagation time from S to P is at the level of  $\sim 10^3$  s, which is much shorter than the time scales of planetary motions. In the case that time-dependent gravitational fields can no longer be neglected, a profound and systematic approach to integrating the light ray equations has been worked out (Kopeikin 1997; Kopeikin & Schäfer 1999; Kopeikin & Mashhoon 2002; Kopeikin et al. 2006; Kopeikin & Makarov 2007; Kopeikin 2009). In

the Shapiro term (6), the index ‘‘A’’ enumerates each body whose gravitational effect needs to be considered.  $r_A$ ,  $\mathbf{r}_A$  and  $\hat{\mathbf{n}}$  are quantities associated with the propagation of the signal and they are

$$\hat{\mathbf{n}} = \frac{\mathbf{x}_P(t_R) - \mathbf{x}_S(t_E)}{|\mathbf{x}_P(t_R) - \mathbf{x}_S(t_E)|}, \quad (7)$$

$$\mathbf{r}_A(t) = \mathbf{x}_S(t_E) - \mathbf{x}_A(t_E) + c\hat{\mathbf{n}}(t - t_E) + \mathcal{O}(\epsilon^2), \quad (8)$$

and

$$\mathbf{r}_{EA} = \mathbf{r}_A(t_E), \quad r_{EA} = |\mathbf{r}_A(t_E)|, \quad \mathbf{r}_{RA} = \mathbf{r}_A(t_R), \quad r_{RA} = |\mathbf{r}_A(t_R)|. \quad (9)$$

Therefore, differentiating (4) and combining it with Equations (2) and (3), we can express Equation (1) as

$$\begin{aligned} \frac{d\tau}{dT} = & 1 + \epsilon \frac{df_1}{dt_E} + \epsilon^2 \left( 1 + \epsilon \frac{df_1}{dt_E} \right) \left\{ \bar{U}(\mathbf{x}_\oplus) + \frac{1}{2} \mathbf{v}_\oplus^2 + \frac{d}{dT} [\mathbf{v}_\oplus \cdot (\mathbf{x}_S - \mathbf{x}_\oplus)] \right\} \\ & - \epsilon^2 \left( 1 + \epsilon \frac{df_1}{dt_E} \right) \left[ \bar{U}(\mathbf{x}_P) + \frac{1}{2} \mathbf{v}_P^2 \right] + \epsilon^3 \frac{df_2}{dt_E} + \mathcal{O}(\epsilon^4). \end{aligned} \quad (10)$$

After integrating it, we can eventually obtain that

$$\tau - T = \Delta t + \Delta T + \Delta\tau + \mathcal{O}(\epsilon^4). \quad (11)$$

Here,  $\Delta t$  is the light time solution accounting for propagation of the signal (Moyer & Yuen 2000; Kopeikin et al. 2011).  $\Delta T$  is the transformation between TCG and TCB at S and it has two components,  $\Delta T = \Delta T_1 + \Delta T_2$ , where  $\Delta T_1$  and  $\Delta T_2$  are respectively associated with the positions and velocities of the geocenter and S. Their expressions are

$$\Delta T_1 = \epsilon^2 \int_{t_E}^{t_R} \left[ \bar{U}(\mathbf{x}_\oplus) + \frac{1}{2} \mathbf{v}_\oplus^2 \right] dt, \quad (12)$$

$$\Delta T_2 = \epsilon^2 \mathbf{v}_\oplus(t_E) \cdot [\mathbf{x}_S(t_E) - \mathbf{x}_\oplus(t_E)]. \quad (13)$$

The term  $\Delta\tau$  is the transformation between TCB and  $\tau$  at P and has the form

$$\Delta\tau = -\epsilon^2 \int_{t_E}^{t_R} \left[ \bar{U}(\mathbf{x}_P) + \frac{1}{2} \mathbf{v}_P^2 \right] dt. \quad (14)$$

By making use of Equation (11), one might carry out time transfer between the times onboard and on the Earth by the transmission of signals. However, in practice, some mathematical works need to be done: one is to solve for  $\Delta t$  from the implicit algebraic Equation (4) and the other is to evaluate the integrals in Equations (12) and (14). They can be worked out in either a numerical or analytic way (e.g. Fukushima 2010). In the present paper, we will adopt an analytic way based on some approximations to handle them. Although the validity of these approximations has to be checked independently, this approach might be used by an onboard computer because of its limited capability to perform calculations.

### 3 ANALYTIC APPROACH FOR THE MODEL

Equation (4) is an implicit algebraic equation of  $t_R$  and  $t_E$ . Taking a quick estimation, we find that, for an orbiter around Mars,  $\Delta t_1$  on the right-hand side of Equation (4) is at the level of  $\sim 10^3$  s and  $\Delta t_2$  is about  $10^{-5}$  s due to the largest contribution from the Sun, i.e.  $\Delta t_2/\Delta t_1 \sim 10^{-8}$ , which means the leading term of Equation (4) is

$$\Delta t \equiv t_R - t_E \approx \Delta t_1 = \epsilon |\mathbf{x}_P(t_R) - \mathbf{x}_S(t_E)|. \quad (15)$$

Depending on the procedure for the time transfer, we can generally write the above equation as

$$\Delta t_1 = \epsilon |\mathbf{x}_P(t_E + \Delta t_1) - \mathbf{x}_S(t_E)| + \mathcal{O}(\epsilon \Delta t_2), \quad (16)$$

or

$$\Delta t_1 = \epsilon |\mathbf{x}_P(t_R) - \mathbf{x}_S(t_R - \Delta t_1)| + \mathcal{O}(\epsilon \Delta t_2). \quad (17)$$

If  $\Delta t_1$  is much less than the time scale of the motion of P, Equation (16) can be Taylor expanded as

$$\mathbf{x}_P(t_E + \Delta t_1) = \mathbf{x}_P(t_E) + \mathbf{v}_P(t_E) \Delta t_1 + \frac{1}{2} \mathbf{a}_P(t_E) \Delta t_1^2 + \mathcal{O}(\Delta t_1^3). \quad (18)$$

Similarly, if  $\Delta t_1$  is much less than the time scale of the motion of S, Equation (17) can be expanded as

$$\mathbf{x}_S(t_R - \Delta t_1) = \mathbf{x}_S(t_R) - \mathbf{v}_S(t_R) \Delta t_1 + \frac{1}{2} \mathbf{a}_S(t_R) \Delta t_1^2 + \mathcal{O}(\Delta t_1^3). \quad (19)$$

Substituting Equations (18) and (19) into (16) and (17) respectively, we can solve them respectively by iteration as

$$\begin{aligned} \Delta t_1 = & \epsilon r_{PS}(t_E) + \epsilon^2 \mathbf{r}_{PS}(t_E) \cdot \mathbf{v}_P(t_E) + \frac{1}{2} \epsilon^3 \left\{ \mathbf{v}_P^2(t_E) r_{PS}(t_E) \right. \\ & \left. + \left[ \mathbf{r}_{PS}(t_E) \cdot \mathbf{a}_P(t_E) \right] r_{PS}(t_E) + \left[ \mathbf{r}_{PS}(t_E) \cdot \mathbf{v}_P(t_E) \right]^2 r_{PS}^{-1}(t_E) \right\} + \mathcal{O}(\epsilon^4), \end{aligned} \quad (20)$$

where  $\mathbf{r}_{PS}(t_E) = \mathbf{x}_P(t_E) - \mathbf{x}_S(t_E)$  and  $r_{PS}(t_E) = |\mathbf{r}_{PS}(t_E)|$ , and

$$\begin{aligned} \Delta t_1 = & \epsilon r_{PS}(t_R) + \epsilon^2 \mathbf{r}_{PS}(t_R) \cdot \mathbf{v}_S(t_R) + \frac{1}{2} \epsilon^3 \left\{ \mathbf{v}_S^2(t_R) r_{PS}(t_R) \right. \\ & \left. - \left[ \mathbf{r}_{PS}(t_R) \cdot \mathbf{a}_S(t_R) \right] r_{PS}(t_R) + \left[ \mathbf{r}_{PS}(t_R) \cdot \mathbf{v}_S(t_R) \right]^2 r_{PS}^{-1}(t_R) \right\} + \mathcal{O}(\epsilon^4), \end{aligned} \quad (21)$$

where  $\mathbf{r}_{PS}(t_R) = \mathbf{x}_P(t_R) - \mathbf{x}_S(t_R)$  and  $r_{PS}(t_R) = |\mathbf{r}_{PS}(t_R)|$ . In the present investigation, we consider  $t_E$  to be a known quantity so that Equation (20) will be used in the rest of this paper. For the term representing the Shapiro delay (6), which is at the post-Newtonian order, we neglect the difference between its dependence on  $t_E$  and  $t_R$ . With the definitions of  $r_{SA}(t_E) = |\mathbf{x}_S(t_E) - \mathbf{x}_A(t_E)|$  and  $r_{PA}(t_E) = |\mathbf{x}_P(t_E) - \mathbf{x}_A(t_E)|$ , we can obtain (Moyer & Yuen 2000; Kopeikin et al. 2011)

$$\Delta t_2 = 2\epsilon^3 G \sum_A m_A \ln \left[ \frac{r_{PA}(t_E) + r_{SA}(t_E) + r_{PS}(t_E)}{r_{PA}(t_E) + r_{SA}(t_E) - r_{PS}(t_E)} \right] + \mathcal{O}(\epsilon^4), \quad (22)$$

in which the time delay caused by the Sun can reach the level of about 10  $\mu\text{s}$ . Finally, Equation (4) can be reduced to

$$\Delta t = \Delta t_1 + \Delta t_2 = \Delta t_L + \Delta t_V + \Delta t_A + \Delta t_S + \mathcal{O}(\epsilon^4),$$

where

$$\Delta t_L = \epsilon r_{PS}(t_E), \quad (23)$$

$$\Delta t_V = \epsilon^2 \mathbf{r}_{PS}(t_E) \cdot \mathbf{v}_P(t_E), \quad (24)$$

$$\begin{aligned} \Delta t_A = & \frac{1}{2} \epsilon^3 \left\{ \mathbf{v}_P^2(t_E) r_{PS}(t_E) + \left[ \mathbf{r}_{PS}(t_E) \cdot \mathbf{a}_P(t_E) \right] r_{PS}(t_E) \right. \\ & \left. + \left[ \mathbf{r}_{PS}(t_E) \cdot \mathbf{v}_P(t_E) \right]^2 r_{PS}^{-1}(t_E) \right\}, \end{aligned} \quad (25)$$

$$\Delta t_S = 2\epsilon^3 G \sum_A m_A \ln \left[ \frac{r_{PA}(t_E) + r_{SA}(t_E) + r_{PS}(t_E)}{r_{PA}(t_E) + r_{SA}(t_E) - r_{PS}(t_E)} \right]. \quad (26)$$

In order to analytically obtain approximate values of the integrals in Equations (12) and (14), we will use the trapezoidal rule (Stoer & Bulirsch 2002) since  $\Delta t$  is much less than the time scales of planetary motions in the solar system. With the help of

$$\bar{U}[\mathbf{x}_\oplus(t_R)] = \bar{U}[\mathbf{x}_\oplus(t_E)] + \epsilon r_{\text{PS}}(t_E) \mathbf{v}_\oplus(t_E) \cdot \nabla \bar{U}[\mathbf{x}_\oplus(t_E)] + \mathcal{O}(\epsilon^2) \quad (27)$$

and

$$\frac{1}{2} \mathbf{v}_\oplus^2(t_R) = \frac{1}{2} \mathbf{v}_\oplus^2(t_E) + \epsilon r_{\text{PS}}(t_E) \mathbf{v}_\oplus(t_E) \cdot \mathbf{a}_\oplus(t_E) + \mathcal{O}(\epsilon^2), \quad (28)$$

we can have

$$\Delta T_1 \approx \frac{1}{2} \epsilon^2 \Delta t \left\{ \bar{U}[\mathbf{x}_\oplus(t_E)] + \frac{1}{2} \mathbf{v}_\oplus^2(t_E) + \bar{U}[\mathbf{x}_\oplus(t_R)] + \frac{1}{2} \mathbf{v}_\oplus^2(t_R) \right\} = I_1 + I_2 + \mathcal{O}(\epsilon^5), \quad (29)$$

where

$$I_1 = \epsilon^3 r_{\text{PS}}(t_E) \left\{ \bar{U}[\mathbf{x}_\oplus(t_E)] + \frac{1}{2} \mathbf{v}_\oplus^2(t_E) \right\}, \quad (30)$$

$$I_2 = \frac{1}{2} \epsilon^4 r_{\text{PS}}^2(t_E) \left\{ \mathbf{v}_\oplus(t_E) \cdot \nabla \bar{U}[\mathbf{x}_\oplus(t_E)] + \mathbf{v}_\oplus(t_E) \cdot \mathbf{a}_\oplus(t_E) \right\}. \quad (31)$$

Applying the same scheme, we can obtain the approximate value of the integral in Equation (14) as

$$\Delta \tau \approx \sigma_1 + \sigma_2 + \mathcal{O}(\epsilon^5), \quad (32)$$

where

$$\sigma_1 = -\epsilon^3 r_{\text{PS}}(t_E) \left\{ \bar{U}[\mathbf{x}_\text{P}(t_E)] + \frac{1}{2} \mathbf{v}_\text{P}^2(t_E) \right\}, \quad (33)$$

$$\sigma_2 = -\frac{1}{2} \epsilon^4 r_{\text{PS}}^2(t_E) \left\{ \mathbf{v}_\text{P}(t_E) \cdot \nabla \bar{U}[\mathbf{x}_\text{P}(t_E)] + \mathbf{v}_\text{P}(t_E) \cdot \mathbf{a}_\text{P}(t_E) \right\}. \quad (34)$$

It is easy to check that  $I_1$  and  $\sigma_1$  are the respective rectangular approximations of  $\Delta T_1$  and  $\Delta \tau$ . After a rough estimation, we find that

$$I_1 \sim \epsilon^2 \Delta t \left( \frac{GM_\odot}{|\mathbf{x}_\odot - \mathbf{x}_\oplus|} + \frac{1}{2} \mathbf{v}_\oplus^2 \right) \sim 13 \left( \frac{\Delta t}{900 \text{ s}} \right) \mu\text{s}, \quad (35)$$

and

$$\sigma_1 \sim -\epsilon^2 \Delta t \left[ \frac{GM_\odot}{|\mathbf{x}_\odot - \mathbf{x}_{\text{Mars}}|} + \frac{1}{2} \mathbf{v}_{\text{Mars}}^2(t_E) \right] \sim -9 \left( \frac{\Delta t}{900 \text{ s}} \right) \mu\text{s}. \quad (36)$$

Combining Equations (35) and (36), we can estimate the leading contribution of  $\Delta T_1 + \Delta \tau$  as

$$\Delta T_1 + \Delta \tau \sim I_1 + \sigma_1 \sim 4 \left( \frac{\Delta t}{900 \text{ s}} \right) \mu\text{s}. \quad (37)$$

The reason that we keep the next-to-leading order terms  $I_2$  and  $\sigma_2$  in Equations (12) and (14) here is to check the self-consistency of our approach (see Sect. 4 for details).

In summary, after the above analytic manipulation, Equation (11) can be written as

$$\tau - T = \Delta t_L + \Delta t_V + \Delta t_A + \Delta t_S + I_1 + \sigma_1 + \Delta T_2 + \mathcal{O}(\epsilon^4), \quad (38)$$

which explicitly depends on  $t_E$ . By assuming there is an Yinghuo-1-like orbiter, we will calculate and show the contributions from various sources in Equation (38).

#### 4 EVALUATION OF THE ANALYTIC MODEL

Taking the Yinghuo-1 Mission (Ping et al. 2010a,b) as a technical example of future Chinese Mars explorations, we will evaluate the significance and contributions of various components in the transformation of Equation (38).

We assume there is a spacecraft orbiting around Mars from 2017 January 1 starting at the time  $00^{\text{h}}00^{\text{m}}00.00^{\text{s}}$  and continuing to 2018 January 1 at  $00^{\text{h}}00^{\text{m}}00.00^{\text{s}}$  under the time scale of the Barycentric Dynamical Time (TDB). Since Pan & Xie (2014) showed that the difference between TCB and TDB contributes only about  $0.2 \mu\text{s}$  to  $\tau - T$  in the time scale of a year, we neglect this difference in our calculation. The origin of all time coordinates is chosen to coincide with  $00^{\text{h}}00^{\text{m}}00.00^{\text{s}}$  on 2017 January 1 in the rest of this paper. The orbital inclination of the spacecraft with respect to the Martian equator is  $5^\circ$ . The apoapsis altitude is 80 000 km and the periapsis altitude is 800 km, with a period of about 3.2 d. In particular, the positions and velocities of celestial bodies are taken from the ephemeris DE405 provided by NASA's JPL and the orbit of the spacecraft is solved by numerically integrating the Einstein-Infeld-Hoffmann equation (Einstein et al. 1938) with the Runge-Kutta 7 method (Stoer & Bulirsch 2002) with the stepsize being one-hundredth of its Keplerian period. In the calculation, we include the gravitational contributions from the Sun, eight planets, the Moon and three large asteroids: Ceres, Pallas and Vesta. We also assume the ground station is in Shanghai, China.

Figure 1 shows the curves of  $\Delta t_{\text{L}}$  (top panel),  $\Delta t_{\text{V}}$  (middle panel) and  $\Delta t_{\text{A}}$  (bottom panel). They can respectively reach the levels of  $\sim 10^3$  s,  $\sim 10^{-2}$  s and  $\sim 10^{-3}$  s. This interrelation of  $\Delta t_{\text{L}} \gg \Delta t_{\text{V}} > \Delta t_{\text{A}}$  is consistent with the limitations imposed on the validity of our analytic approach. Some features appear like spikes in the middle and bottom panels of Figure 1. These spike-like appearances are caused by the low resolution of the figure. We enlarge one of these “spikes” in the middle panel and replot it in the sub-figure(a) of Figure 1. It clearly shows the curve of  $\Delta t_{\text{V}}$  changes fast and smoothly due to the orbital motion of the spacecraft around Mars with a period of 3.2 d. This is also shown in the sub-figure(b) of Figure 1, which displays a single “spike” in the bottom panel of  $\Delta t_{\text{A}}$ . The effects of the Shapiro time delay  $\Delta t_{\text{S}}$  caused by various gravitational bodies are shown in Figure 2. Among them, the Sun provides the largest contribution, which is at the level of  $\sim 10 \mu\text{s}$ .

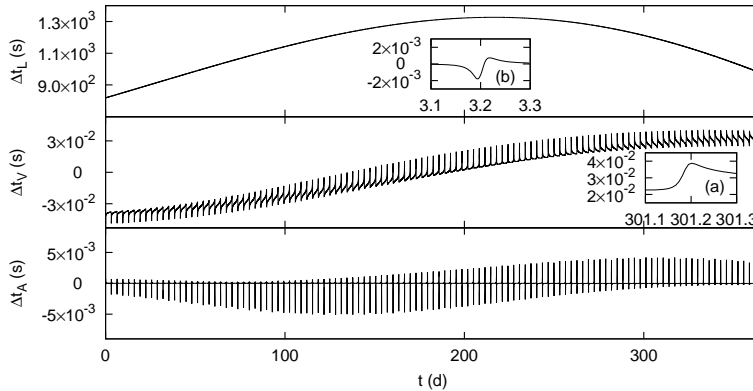


**Fig. 1** Curves of  $\Delta t_{\text{L}}$  (top panel),  $\Delta t_{\text{V}}$  (middle panel) and  $\Delta t_{\text{A}}$  (bottom panel). One of the “spikes” in the middle panel is enlarged and re-plotted in sub-figure (a), which shares the same scales and units as the middle panel. Sub-figure(a) clearly shows that the curve of  $\Delta t_{\text{V}}$  changes fast and smoothly due to the orbital motion of the spacecraft around Mars with a period of 3.2 d. Sub-figure(b) shows a single “spike” in the bottom panel of  $\Delta t_{\text{A}}$  and it has the same scales and units as in the bottom panel.

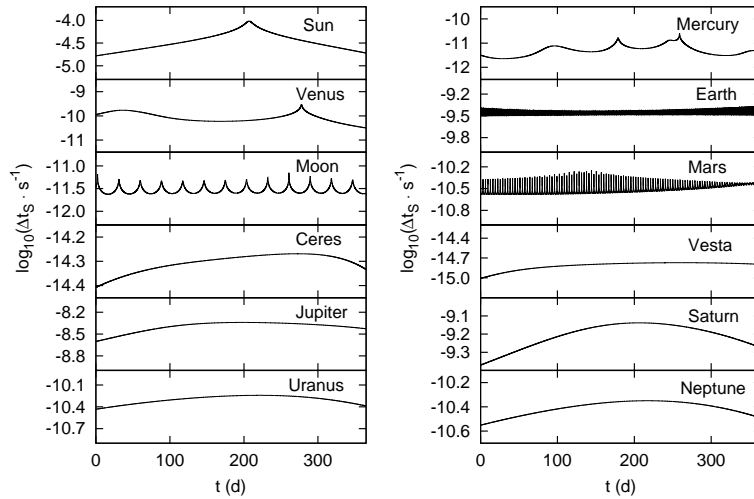


**Fig. 2** The effects of the Shapiro time delay  $\Delta t_S$  caused by different gravitational bodies. The black strip in the panel representing Earth is because of the change in position of the station due to the Earth’s rotation, which makes the curve have a fast oscillation with a period of a day. All of the “spikes” and “tips” in some panels are caused by the low resolution. They will look smooth when they are enlarged and shown in a figure with a higher resolution (see Fig. 1(a) and (b) for examples).

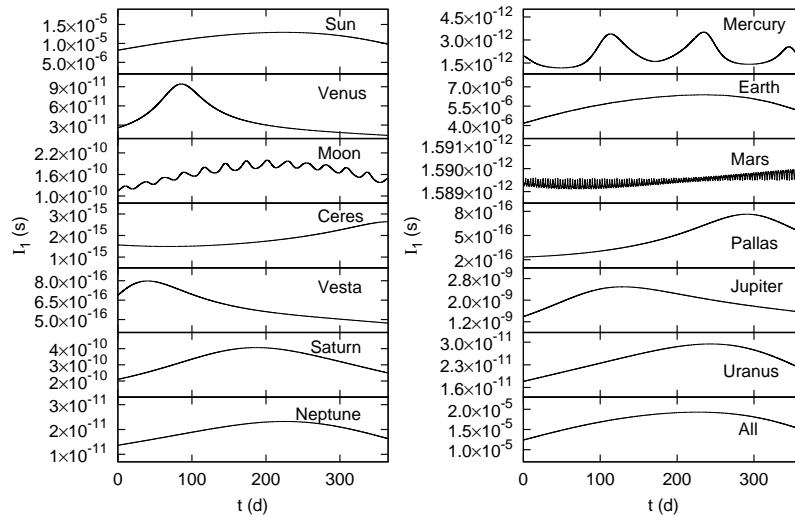


**Fig. 3** The effects of  $I_1$  caused by different gravitational bodies and its overall contribution. All of the “spikes” in the panel of Mars are caused by the low resolution. They would look smooth when they are enlarged and shown in a figure with a higher resolution (see Fig. 1(a) and (b) for examples).

The black strip in the panel representing Earth in Figure 2 is because of the change in position of the station due to Earth’s rotation, which makes the curve have a period of a day.

Figures 3 and 5 respectively represent the contribution of  $I_1$  and  $\sigma_1$ . Their magnitudes of  $\sim 15 \mu s$  and  $\sim -10 \mu s$  agree with our estimated values given by Equations (35) and (36). The contributions of the Sun and P dominate the outcomes of  $I_1$  and  $\sigma_1$ . Again, the black strip in the panel representing

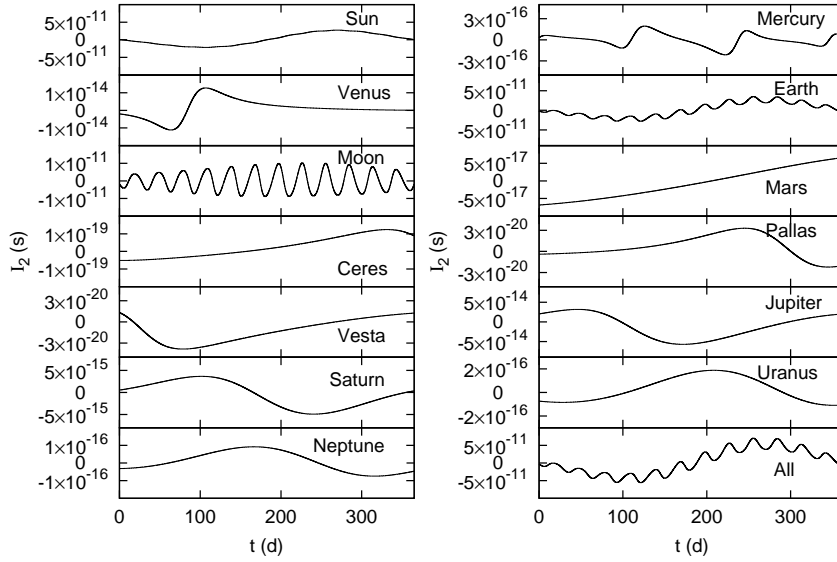


**Fig. 4** The effects of  $I_2$  caused by different gravitational bodies and its overall contribution.

Earth in Figure 5 is caused by the change in position of the station due to Earth's rotation with a period of a day. As a check of the self-consistency of our analytic approach, their next-to-leading order corrections  $I_2$  and  $\sigma_2$  are shown in Figures 4 and 6 and they are at least ten times less than  $I_1$  and  $\sigma_1$ . Like the "spikes" appearing in Figure 1, some "spikes" and "tips," where derivatives of the function seem to be discontinuous, can also be seen in Figures 2, 3, 5 and 6. However, all these "spikes" and "tips" are likewise caused by the low resolutions of the figures. They would look smooth when they are enlarged and shown in figures with higher resolutions (see Fig. 1(a) and (b) for examples).

The term  $\Delta T_2$  in Equation (13) depends on the location of S. If we consider a tracking station on the ground,  $\Delta T_2$  will show a strong effect caused by the rotation of the Earth, which can reach the level of about  $2 \mu\text{s}$  with a period of a day (see a similar figure like the sub-figure in the bottom right corner of fig. 3 in Pan & Xie (2014)). In the calculation, we take the direction of the pole of rotation and the prime meridian of the Earth from the report of the IAU Working Group on Cartographic Coordinates and Rotational Elements (Archinal et al. 2011), which is a good enough approximation for our purposes.

The leading magnitudes of these components are summarized in Table 1.

**Table 1** Maximum Contributions of Components in Eq. (38)

Components	Level ( $\mu\text{s}$ )
$\Delta t_L$	$10^9$
$\Delta t_V$	$10^4$
$\Delta t_A$	$10^3$
$\Delta t_S$	10
$I_1$	15
$\sigma_1$	-10
$\Delta T_2$	2

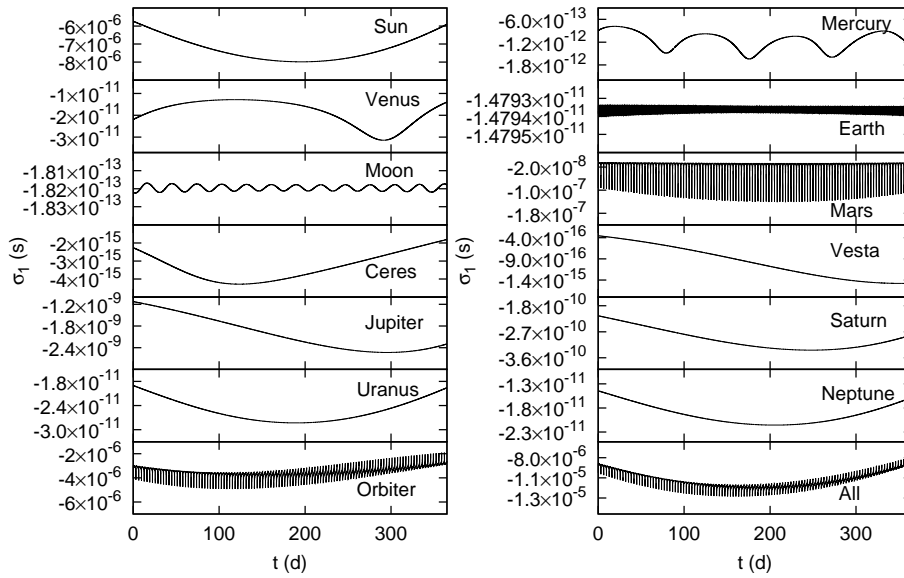


**Fig. 5** The effects of  $\sigma_1$  caused by different gravitational bodies and the orbiter and its overall contribution. The black strip in the panel representing Earth is because of the change in position of the station due to the Earth’s rotation, which makes the curve have a fast oscillation with a period of a day. All of the “spikes” in some panels are caused by the low resolution. They would look smooth when they are enlarged and shown in a figure with a higher resolution (see Fig. 1(a) and (b) for examples).

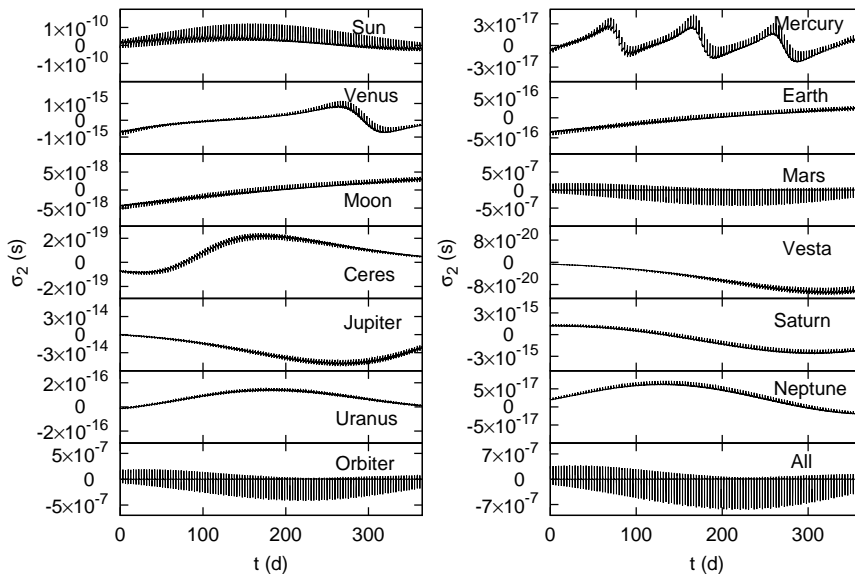


**Fig. 6** The effects of  $\sigma_2$  caused by different gravitational bodies and the orbiter and its overall contribution. All of the “spikes” in some panels are caused by the low resolution. They would look smooth when they are enlarged and shown in a figure with a higher resolution (see Fig. 1(a) and (b) for examples).

## 5 CONCLUSIONS AND DISCUSSION

In this work, we take an Yinghuo-1-like mission as an example and investigate the relativistic algorithm for time transfer between the proper time  $\tau$  of the onboard clock and TCG, which extends previous works (Deng 2012; Pan & Xie 2013, 2014) by including the effects of the propagation of light signals. In order to evaluate the implicit algebraic equations and integrals in the model, we take an analytic approach to work out their approximate values. The analytic model (see Equation (38)) might be used for an onboard computer because of its limited capability to perform calculations. We find that the contributions of the Sun, the ground station and the spacecraft dominate the outcomes of the relativistic corrections to the model.

**Acknowledgements** This work is funded by the National Natural Science Foundation of China (Grant Nos. 11103010 and J1210039), the Fundamental Research Program of Jiangsu Province of China (No. BK2011553) and the Research Fund for the Doctoral Program of Higher Education of China (No. 20110091120003).

## References

- Archinal, B. A., A'Hearn, M. F., Bowell, E., et al. 2011, *Celestial Mechanics and Dynamical Astronomy*, 109, 101
- Bertotti, B., Iess, L., & Tortora, P. 2003, *Nature*, 425, 374
- Cacciapuoti, L., & Salomon, C. 2009, *European Physical Journal Special Topics*, 172, 57
- Christophe, B., Andersen, P. H., Anderson, J. D., et al. 2009, *Experimental Astronomy*, 23, 529
- Christophe, B., Spilker, L. J., Anderson, J. D., et al. 2012, *Experimental Astronomy*, 34, 203
- Deng, X.-M. 2012, *RAA (Research in Astronomy and Astrophysics)*, 12, 703
- Deng, X.-M., & Xie, Y. 2013a, *RAA (Research in Astronomy and Astrophysics)*, 13, 1225
- Deng, X.-M., & Xie, Y. 2013b, *MNRAS*, 431, 3236
- Deng, X.-M., & Xie, Y. 2014, *RAA (Research in Astronomy and Astrophysics)*, 14, 319
- Einstein, A., Infeld, L., & Hoffmann, B. 1938, *Annals of Mathematics*, 39, 65
- Fukushima, T. 2010, in *IAU Symposium*, 261, eds. S. A. Klioner, P. K. Seidelmann, & M. H. Soffel, 89
- Jensen, J. R., & Weaver, G. L. 2007, in *Proc. 39th Annual Precise Time and Time Interval (PTTI) Meeting*, 79
- Kopeikin, S., Efroimsky, M., & Kaplan, G. 2011, *Relativistic Celestial Mechanics of the Solar System*, eds. S. Kopeikin, M. Efroimsky, & G. Kaplan (Wiley)
- Kopeikin, S., Korobkov, P., & Polnarev, A. 2006, *Classical and Quantum Gravity*, 23, 4299
- Kopeikin, S., & Mashhoon, B. 2002, *Phys. Rev. D*, 65, 064025
- Kopeikin, S. M. 1997, *Journal of Mathematical Physics*, 38, 2587
- Kopeikin, S. M. 2009, *MNRAS*, 399, 1539
- Kopeikin, S. M., & Makarov, V. V. 2007, *Phys. Rev. D*, 75, 062002
- Kopeikin, S. M., Polnarev, A. G., Schäfer, G., & Vlasov, I. Y. 2007, *Physics Letters A*, 367, 276
- Kopeikin, S. M., & Schäfer, G. 1999, *Phys. Rev. D*, 60, 124002
- Landau, L. D., & Lifshitz, E. M. 1975, *The Classical Theory of Fields* (4th edn.; Oxford: Pergamon Press)
- Misner, C. W., Thorne, K. S., & Wheeler, J. A. 1973, *Gravitation* (San Francisco: W. H. Freeman and Co.)
- Moyer, T. D., & Yuen, J. H. 2000, *Formulation for Observed and Computed Values of Deep Space Network Data Types for Navigation* (Jet Propulsion Laboratory, National Aeronautics and Space Administration)
- Nelson, R. A. 2011, *Metrologia*, 48, 171
- Pan, J.-Y., & Xie, Y. 2013, *RAA (Research in Astronomy and Astrophysics)*, 13, 1358
- Pan, J.-Y., & Xie, Y. 2014, *RAA (Research in Astronomy and Astrophysics)*, 14, 233
- Petit, G., & Wolf, P. 2005, *Metrologia*, 42, 138
- Ping, J. S., Qian, Z. H., Hong, X. Y., et al. 2010a, in *Lunar and Planetary Science Conference*, 41, 1060

- Ping, J.-S., Shang, K., Jian, N.-C., et al. 2010b, in Proceedings of the Ninth Asia-Pacific International Conference on Gravitation and Astrophysics, eds. J. Luo, Z.-B. Zhou, H.-C. Yeh, & J.-P. Hsu, 225
- Samain, E. 2002, in EGS General Assembly Conference Abstracts, 27, 5808
- Shapiro, I. I. 1964, Physical Review Letters, 13, 789
- Soffel, M., Klioner, S. A., Petit, G., et al. 2003, AJ, 126, 2687
- Stoer, J., & Bulirsch, R. 2002, Introduction to Numerical Analysis (New York: Springer)
- Wolf, P., Bordé, C. J., Clairon, A., et al. 2009, Experimental Astronomy, 23, 651